A FEM-based model to study the behaviour of corroded RC beams shear-repaired by NSM CFRP rods technique

Belal Almassri, Joaquim A.O. Barros, Firas Al Mahmoud, Raoul François

A FEM-based model to study the behaviour of corroded RC beams shear repaired by NSM CFRP rods technique

Belal ALMASSRI (1), Joaquim A.O. BARROS (2), Firas AL MAHMOUD (3), Raoul FRANCOIS (1)

(1) *Université de Toulouse; UPS, INSA, LMDC (Laboratoire Matériaux et Durabilité des Constructions), Toulouse, France*

(2) *ISISE, Dep. Civil Eng., Minho University, Guimarães, Portugal*

(3) *Institut Jean Lamour, UMR 7198, CNRS, Université de Lorraine, Nancy, France*

Keywords: corrosion, repair, RC beams, NSM CFRP rods, FEM, shear.

Corresponding author: Belal Almassri Tel.: (+33)561559933. E-mail address: almassri@etud.insa-toulouse.fr

ABSTRACT

This paper presents the main features of finite element FE numerical model developed using the computer code FEMIX to predict the near-surface mounted NSM carbon-fiber-reinforced polymer CFRP rods shear repair contribution to corroded reinforced concrete RC beams. In the RC beams shear repaired with NSM technique, the Carbon Fibre Reinforced Polymer (CFRP) rods are placed inside pre-cut grooves onto the concrete cover of the RC beam's lateral faces and are bonded to the concrete with high epoxy adhesive. Experimental and 3D numerical modelling results are presented in this paper in terms of load-deflection curves, and failure modes for 4 short corroded beams: two corroded beams (A1CL3-B and A1CL3-SB) and two control beams (A1T-B and A1T-SB), the beams noted with B were let repaired in bending only with NSM CFRP rods while the ones noted with SB were repaired in both bending and shear with NSM technique. The corrosion of the tensile steel bars and its effect on the shear capacity of the RC beams was discussed. Results showed that the FE model was able to capture the main aspects of the experimental load-deflection curves of the RC beams, moreover it has presented the experimental failure modes and FE numerical modelling crack patterns and both gave similar results for non-shear repaired beams which failed in diagonal tension mode of failure and for shear-repaired beams which failed due to large flexural crack at the middle of the beams along with the concrete crushing, three dimensional crack patterns were produced for shear-repaired beams in order to investigate the splitting cracks occurred at the middle of the beams and near the support.

1. Introduction

The deterioration of reinforced concrete (RC) structures is a serious issue for many nations, as it could put the public safety in jeopardy and the escalating repair cost could directly burden the future economy (1), the corrosion of steel reinforcement is still one of the major concerns as it may lead to significant reduction in terms of ultimate capacity and serviceability of the RC structures (2,3). Many studies presented the steel corrosion effect on the flexural behavior of the RC structures (4–7), on the other hand very few studies showed the corrosion effect on the shear capacity of the RC structures. Moreover, most of the available literature (8–10) studied the corrosion effect on the shear behavior of the RC beams throughout using impressed current induced corrosion to the steel bars. As these accelerated systems do not represent the real state of corroded structures, very few studies aimed at studying the natural corroded structures, these studies were based on long-term natural corrosion systems (11,12) in which the RC beams were stored in chloride environment under service loads.

Near surface mounted (NSM) with carbon fibre reinforced polymer (CFRP) rods is a promising strengthening technique to increase the shear resistance of RC beams that have some risk of collapsing in a brittle shear failure mode. Shear strengthening of RC beams by NSM CFRP rods technique consists of fixing the CFRP rods with a high performance epoxy adhesive into thin grooves cut onto the concrete cover of the RC beam's lateral faces, several experimental based studies investigated the efficiency of using the NSM CFRP rods technique in shear strengthening of the RC beams (13–15). Other studies used the NSM CFRP laminates (strips) instead of round bars to study the effect of the NSM technique on the shear capacity of the RC beams (16,17). Nanni et al. (18) predicted the contribution of NSM systems to the shear resistance of RC beams but this prediction was based on the assumption that the laminates debonding is the dominant mode of failure. On the other hand, the separation of the concrete cover containing the laminates is always more frequently reported in relevant studies (15,19). Bianco et al. (20) produced an analytical model which is able to predict the NSM CFRP laminates contribution to the shear strength based on different possible modes of failure: loss of bond debonding; concrete semiconical tensile fracture; mixed shallow-semicone-plus-debonding; and strip tensile fracture.

NSM technique to repair corroded RC beams was hardly studied. Bending strengthening is mainly concerned and only a very recent paper (21) studied the NSM effect on the experimental shear behavior of the corroded RC beams.

The available research showed that the predictive performance of computer programs based on the finite element method (FEM) for the nonlinear analysis of RC structures failing in shear is very related to the constitutive model used to simulate the shear stress transfer in the cracked concrete (22,23), Suryanto et al. (23) mentioned that it is significantly required to take into account the shear stress- strain softening law for concrete in order to capture the real damage which happens in the concrete during the cracking process. There are some available studies (24–26) that used the FE modelling programs to study the effect of using NSM technique in shear strengthening of RC beams, a multi-directional fixed smeared crack model was implemented by Barros et al. (26) in order to simulate the CFRP strengthened RC beams failing in shear and flexure. Barros et al. (19) investigated the effectiveness limitations of the NSM CFRP laminates technique in shear strengthening of the RC beams using the computer code FEMIX and reasoned that for the concrete tensile strength as some of the concrete volume failed here was attached to the CFRP laminates.

There are no available numerical modelling studies which were made to investigate the mechanical behavior and failure modes of the corroded RC beams repaired in shear with NSM CFRP rods. This paper studies the performance of corroded short-span reinforced concrete beams repaired with the NSM FRP technique throughout implementing FE model using the computer code FEMIX. Some of the beams were repaired in bending only and the others were repaired in bending and shear. All beams were tested experimentally in three-point loading up to failure. The FE models investigate the failure modes and the shear capacities for all RC beams, the shear capacity of the short-span corroded beams repaired in shear and bending was compared to that of similar non-repaired beams.

2. Experimental programme

2.1 Experimental procedure

An experimental program was started at LMDC (Laboratory of Materials and Durability of Constructions) in 1984 aimed at understanding the effects of the steel corrosion on the structural behavior of the RC elements. Many experimental studies were conducted on those beams to evaluate the development of corrosion cracking, to measure chloride content and to analyse the change of the mechanical behaviour (27,28). The natural aggressive environment system details can be found elsewhere (29).

The four (80cm) RC beams studied in this paper were cut of two long beams; two short corroded beams were extracted of the corroded long RC beam (A1CL3-R) and two control

beams were extracted of the control (non-corroded) long RC beam (A1T-R), the two full span length beams were repaired with one 6mm diameter CFRP rod in bending and tested in three points loading up to failure, more details of the long beams can be found elsewhere (30). Two short RC beams; one corroded A1CL3-SB and one control A1T-SB were shear repaired by NSM CFRP rods while two others; one corroded A1CL3-B and A1T-B were kept repaired in bending only. The reinforcement layout of the full length beams and the four short beams is shown in Figure 1.

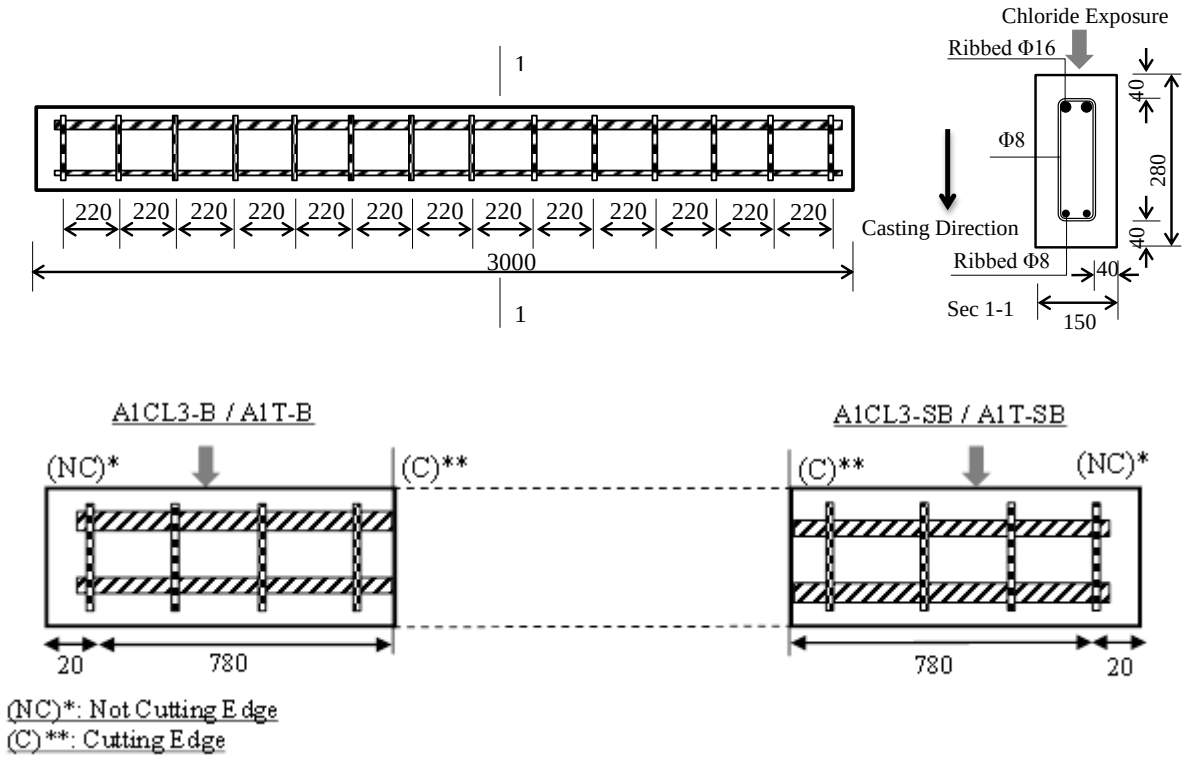

Figure 1 Reinforcement layout all beams. Dimensions are in mm

2.2 Main experimental results

2.2.1 Corrosion results

After the tensile steel bars and steel stirrups extracted of the two corroded beams and cleaned with Clark's solution ANSI/ASTM G1-72, the diameter loss was calculated from a mass weight loss method because the high scatter in the corrosion shape do not allow to measure it directly using a Vernier calliper. According to the corrosion pattern, short pieces of corroded steel bars were cut and weighted to measure the loss of mass due to corrosion. Figure 2 shows the maximum diameter loss found in the A1CL3-B beam was 18% while for A1CL3-SB was 9%.

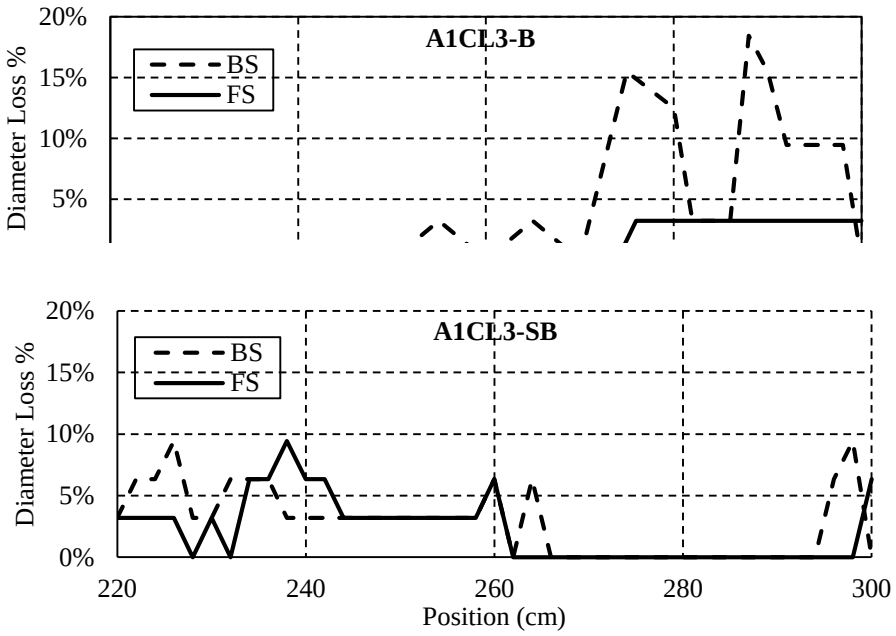

Figure 2 Diameter loss percentages of longitudinal tensile steel bars for corroded beams

For the corroded beam A1CL3-R, the steel stirrups were numbered to indicate the part of the beam they came from and their position in that part (the first number represents the part of the beam and the second number represents the number of the stirrup) as shown in figure 3 which presents also the stirrups numbers of non-repaired corroded RC beam A2CL2-A studied by Dang et al. (31), which will be used as a comparison:

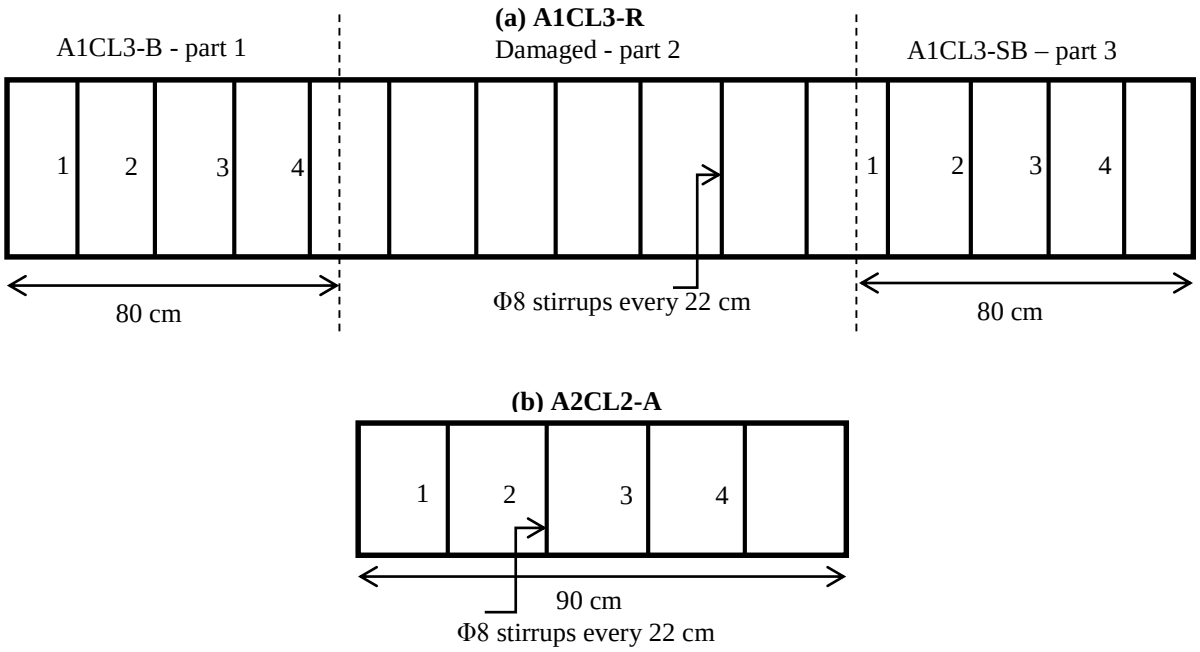

Figure 3 Stirrups numbers of corroded beams (a) A1CL3-R (b) A2CL2-A

Figure 4 (a) shows the locations of corrosion in the steel stirrups and the diameter values for the corroded beam A1CL3-R. No corrosion was found at stirrups 1-1 and 1-2, the maximum diameter loss found in beam A1CL3-B was 63 % at stirrup 1-4 (at the far edge of the diagonal shear crack) while the maximum loss in A1CL3-SB was 38 % at stirrup 3-1. Figure 4 shows also the corrosion map (diameter loss %) for corroded beam A2CL2-A, the maximum diameter loss found 77% (1.84 mm) at the edge where the diagonal shear crack happened.

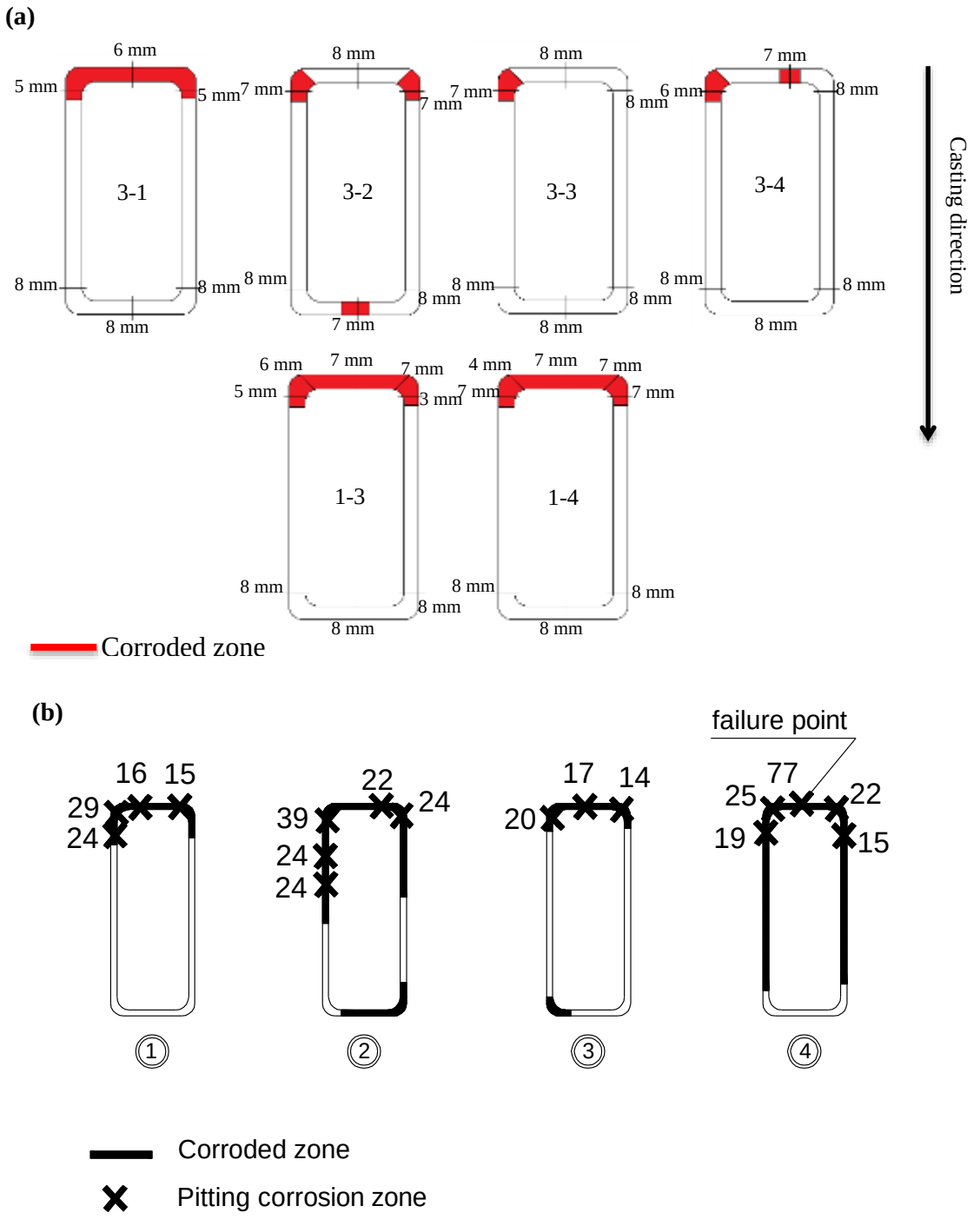

Figure 4 Stirrups corrosion maps (a) diameter in mm for A1CL3-R (b) diameter loss % in A2CL2-A

2.2.2 Ultimate load capacity and modes of failure

The four tested RC beams were compared to other two beams; one is corroded A2CL2-A and the other is control tested by Dang et al. (31), Figure 5 shows the load-deflection curves for all short beams tested experimentally. The shear strengthening increased the shear capacity for the control beams, while the response of the corroded beams due to shear strengthening depends on the pattern and the intensity of steel corrosion.

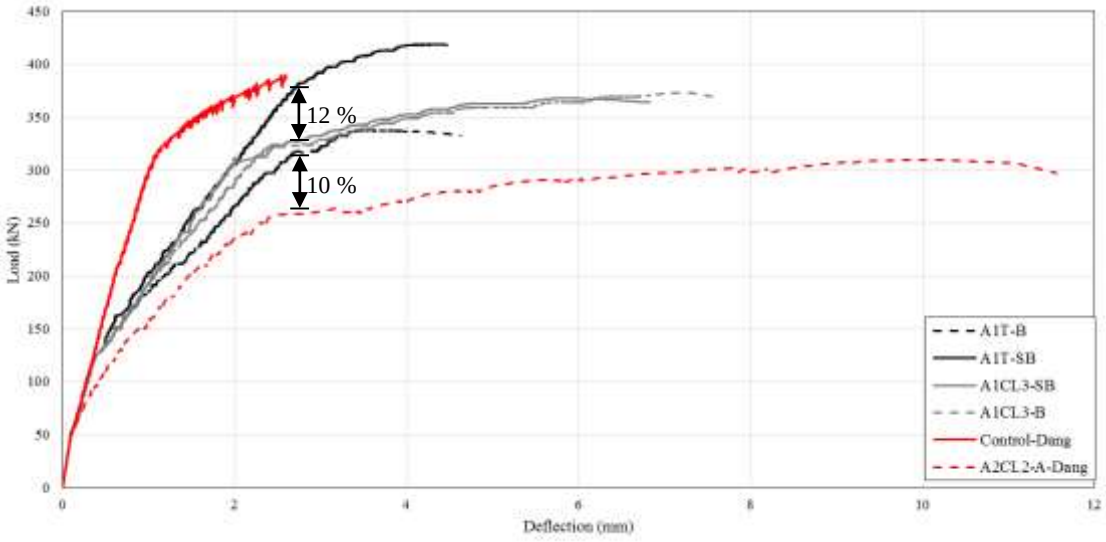

Figure 5 Load-deflection curves for all beams

The difference in the yielding capacity of the shear repaired control beam A1T-SB and the shear repaired corroded beam A1CL3-SB refers to the 12% loss in cross section found at the middle of the corroded beam A1CL3-SB (the load-induced crack occurs at mid-span), while the decrease in the yielding capacity for non-shear repaired corroded beam A2CL2-A in comparison with non-shear repaired beams (Control, A1T-B and A1CL3-B) refers to the 10% loss in cross section found at the edge of the corroded beam A2CL2-A (the same edge of diagonal shear crack) (31).

Experimental results showed also that shear strengthening with NSM CFRP rods technique changed the mode of failure from diagonal crack failure close to support due to slipping of tensile re-bars at anchorage (for non-shear-repaired beams A1T-B and A1CL3-B), to large flexural crack at mid span followed by concrete crushing (for shear-repaired beams A1T-SB and A1CL3-SB) as shown in figure 6.

Figure 6 Experimental modes of failure for all tested beams

It is also noteworthy that for shear-repaired beams A1T-SB and A1CL3-SB, many splitting cracks occurred at the mid-way of the beam's width as shown in figure 7 , these splitting cracks were clear to notice at the bottom of the beam and at the beams edges near the supports. More details of the experimental program of the short beams and experimental results can be found elsewhere (21).

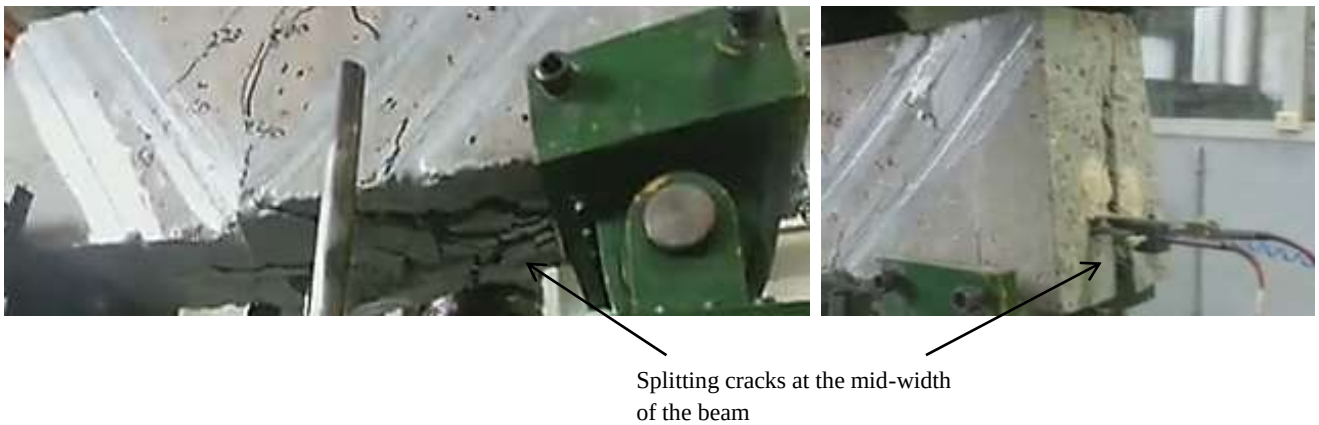

Figure 7 Tensile steel bars slip occurred in non-shear repaired beams A1T-SB and A1CL3-SB

3. Numerical model

In this study, a multi-directional fixed smeared crack model is used to simulate the RC beams failing in shear. The main important aspect in this constitutive model is using the concrete fracture mode I & II by taking into account a softening diagram in order to simulate the crack shear stress vs. crack shear sliding in the context of a smeared approach. The description of the formulation of the multi-directional fixed smeared crack model is restricted to the case of cracked concrete. This model is described in much detail elsewhere (19).

3.1 Concrete Properties

Three dimensional 20 nodes (quadratic) solid elements were used to simulate the concrete material in this numerical model; the concrete properties used are shown in Table 1.

Table 1 Concrete properties

Poisson's ratio	vc = 0.20
Initial Young's modulus	Ec = 30 000 N/mm2
Compressive strength	fc = 60 N/mm2
Tri-linear tensile-softening diagram	fct = 4.5 N/mm2 , Gf' = 0.05 N/mm ξ1 = 0.005, α1 = 0.5, ξ2 = 0.3, α2 = 0.2
Parameter defining the mode I fracture energy available to the new crack	P2 = 1
Shear softening parameters	$\tau_{t,p}^{cr}$= 3 N/mm2, Gf,s = 0.1 N/mm, ß = 0.1
Threshold angle	αth = 30º
Maximum number of cracks per integration points	2

3.1.1 Fracture mode I for concrete "tension softening of concrete"

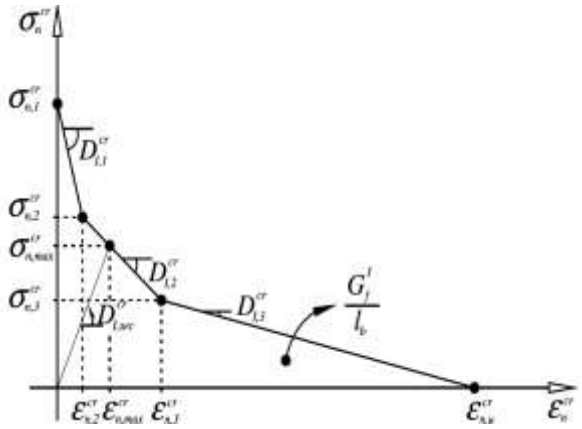

Figure 8 RC fracture mode I "tri-linear tension softening diagram"

The crack evolution in fracture mode I is simulated using a tri-linear tension softening or stiffening diagram as shown in figure 8. In structures controlled by flexural modes of failure, there would be no need to adopt a softening crack shear stress vs. crack shear strain relationship in the numerical model.

3.1.2 Fracture mode II for concrete "Shear softening of concrete"

Suryanto et al. (23) showed that taking into account the shear softening law for modelling the shear stress transfer in cracked concrete is fundamental in order to get better simulation of the behaviour of engineered cement composites (ECC) beams failing in shear. Therefore in this paper a linear shear softening law (shown in figure 9) for modelling the fracture mode II of cement based materials is used.

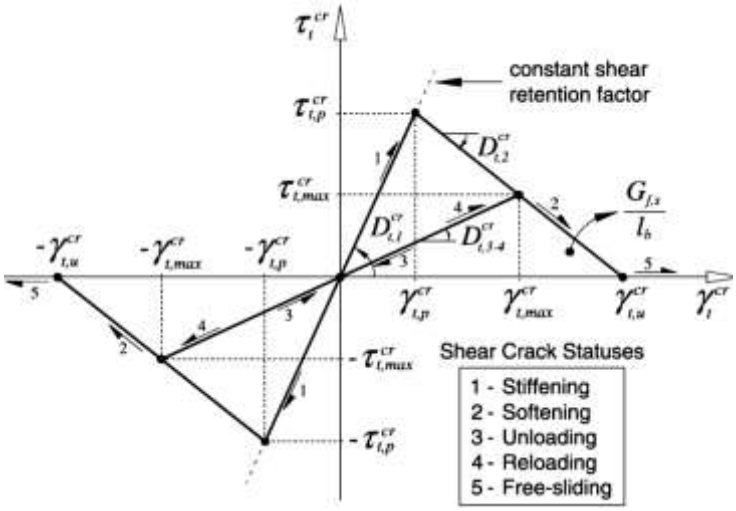

Figure 9 RC fracture mode II "linear shear softening diagram"

3.2 Steel properties

The steel reinforcement bars were implemented here in this model as elastic- plastic behavior. A Poisson's ratio of 0.3 is used while the elastic modulus and yield strength values of steel reinforcement bars and stirrups are used as in Table 2 for both control and corroded steel bars. The post yielding hardening behavior of control and corroded steel bars and steel stirrups is modeled as shown in figure 10 and 11 respectively. Corrosion did not modify the actual yield strength and hardly modified the actual ultimate strength (32,33) but it decreases strongly the ultimate elongation (34–37).

Table 2 Average values of steel bars properties

Specimen Type	Young's modulus (GPa)	Yield Strength (MPa)	Ultimate Strength (MPa)	Ultimate Strain
Non-corroded steel specimen	200	550	604	0.08
Corroded steel specimen	200	550	645	0.04

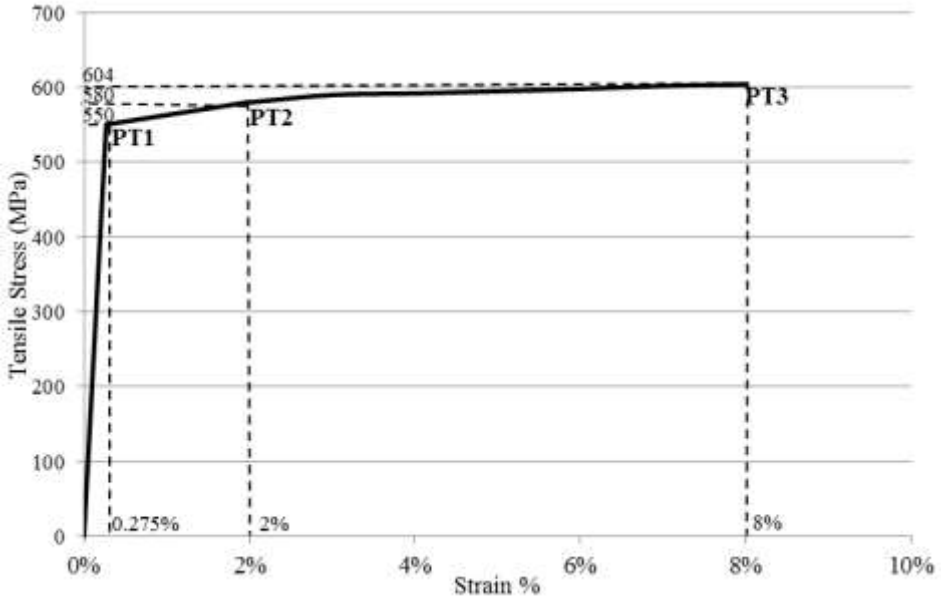

Figure 10 uniaxial constitutive model of non-corroded steel bars

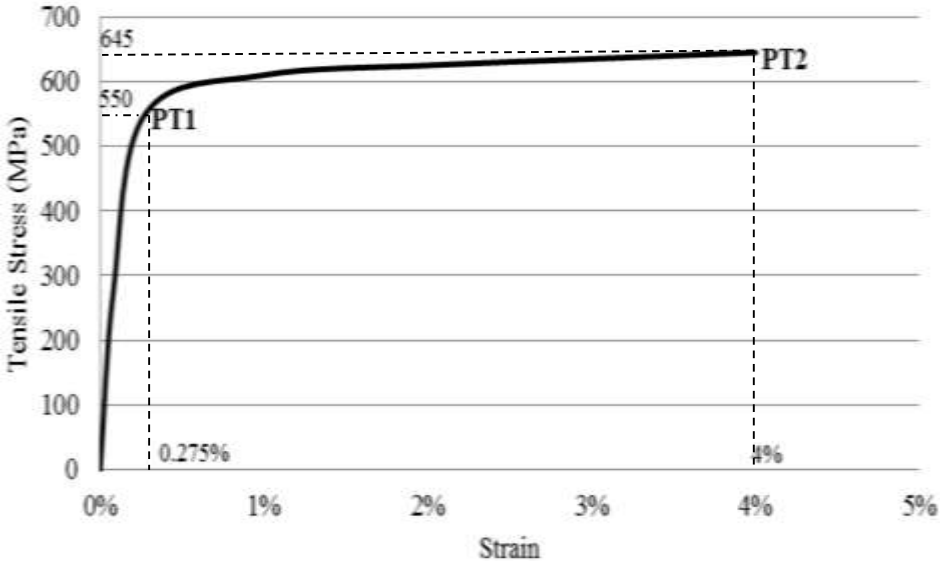

Figure 11 uniaxial constitutive model of corroded steel bars

3.3 CFRP properties

For modelling the NSM CFRP rods, a linear elastic stress– strain relationship was implemented. Table 3 presents the values used in constitutive model for CFRP rods according to the manufacturer's specifications.

Table 3 CFRP rods characteristics.

Type of test	Ultimate strength (MPa)	Modulus of Elasticity (MPa)
Manufacturer's test	2300	150000

3.4 Modelling of RC beams bending and shear repaired with NSM CFRP rods (A1CL3-SB and A1T-SB)

The main objective of this part is to create a reliable numerical model which can simulate and predict the global behavior (load-deflection curves and modes of failure) of two RC beams repaired in shear with NSM CFRP rods (one beam is corroded A1CL3-SB and one is control A1T-SB) both beams were already repaired with NSM CFRP rod in bending as they were extracted out of full length beams A1CL3-R and A1T-R, the two long beams were tested by (30). To simulate the concrete in the beams, three dimensional solid 20-node elements with 3 ×3 Gauss-Legendre integration type were used. The steel bars and stirrups reinforcements, as well as the CFRP rods, were simulated using 3-node quadratic three dimensional embedded cable elements with two Gauss-Legendre integration points. The epoxy adhesive material was not implemented in this model as some previous study (24) showed that the epoxy adhesive has a negligible effect on the global behavior of the RC beams. Figures 12 and 13 show the geometry, elements mesh, loading and supports configuration.

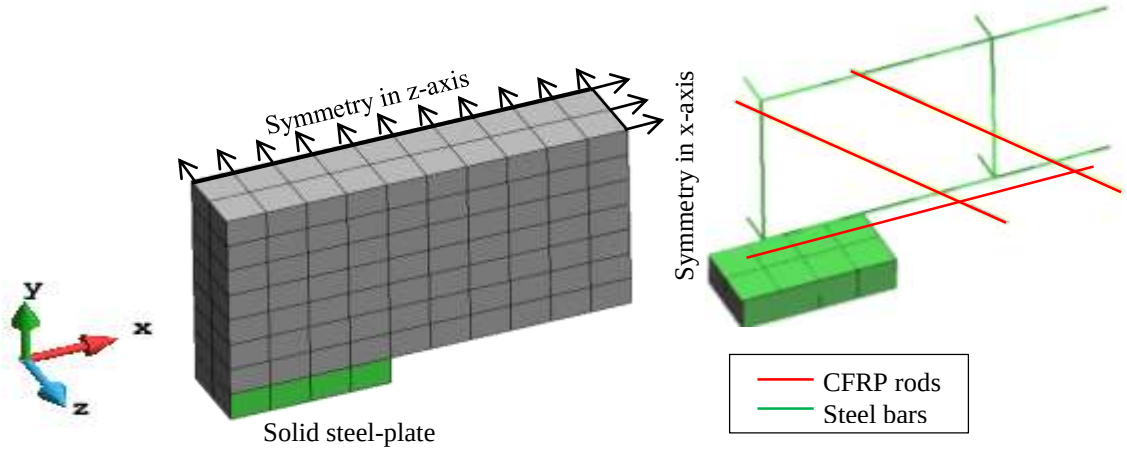

Figure 12 The boundary conditions of the 3D model in an isometric plane in GiD-FEMIX

In order to avoid the elements distortion that could happen as a reason of the point load in the FE numerical model, an edge load is implemented here in this model as shown in figure 13. Moreover, in all numerical models the edge load was applied by direct displacement-control at the point located in the lower right corner of the mesh.

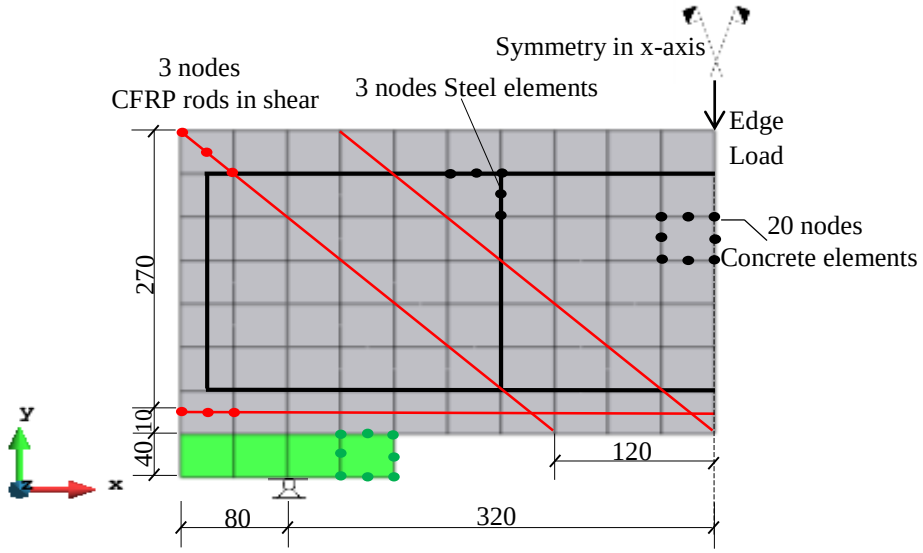

Figure 13 Geometry in (mm), mesh, loading and support conditions in x-y plane for shear repaired beams with NSM CFRP rods

3.4.1 Modelling of corroded RC beam A1CL3-SB

In this numerical model the diameter loss at the middle of the beam (6%) found in tensile steel bars of the corroded beam A1CL3-SB (see figure 2) was used as a constant residual re-bars cross section all along the RC beam. The reduced cross-sectional area at mid-span point was used for this beam as the failure mode recorded experimentally for this beam was due to large crack at the middle of the beam.

3.5 Modelling of RC beams non-shear repaired with NSM CFRP rods (A1CL3-B, A1T-B and A2CL2-A)

One FEM model was implemented for the non-shear-repaired beams with NSM CFRP rods, the model is taking into account the cross sectional area reduction due to steel corrosion for both tensile steel bars and steel stirrups at the failure location, the same numerical modeling properties of the fracture modes parameters for the concrete were used here also, moreover the FE model takes into account two different constitutive steel models (one for corroded beams and one for control beams), figure 14 shows the geometry, elements mesh, loading and

supports configuration for the two beams non-shear-repaired with NSM CFRP rods A1CL3-B , A1T-B and A2CL2-A.

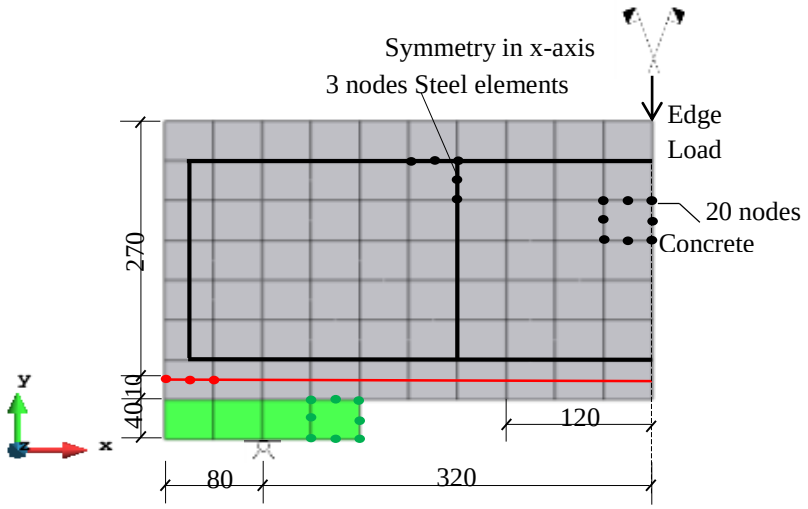

Figure 14 Geometry in (mm), mesh, loading and support conditions in x-y plane for non-shear-repaired beams with NSM CFRP rods

4. Numerical modelling results

4.1 Load-deflection curves and failure modes for RC beams non-shear repaired with NSM CFRP rods (A1CL3-B, A1T-B and A2CL2-A)

One FE model was used for both beams A1CL3-B and A1T-B as no remarkable steel corrosion (neither in tensile steel bars nor in steel stirrups) was found at the edge of the corroded beam A1CL3-B (the same diagonal shear crack edge),. The FE model was used again for the corroded beam A2CL2-A (tested experimentally by Dang et al. (31)) using the 10% loss of tensile steel bars cross section due to corrosion which was found at the edge of the beam (the same diagonal shear crack edge) as a constant residual re-bars cross section all along the RC beam, moreover the steel stirrups diameter found at the failure point of the corroded beam A2CL2-A which was 1.84 mm (77% of diameter loss shown in figure 4(b)) was used in this model as a constant residual cross section for all of the steel stirrups in the RC beam. For A2CL2-A modelling, the uniaxial constitutive law of corroded steel (shown in figure 11) was used. The load-deflection curves for the FE numerical model for the three non-shear-repaired beams A1CL3-B, A1T-B and A2CL2-A were drawn with the experimental load-deflection curves in figure 15.

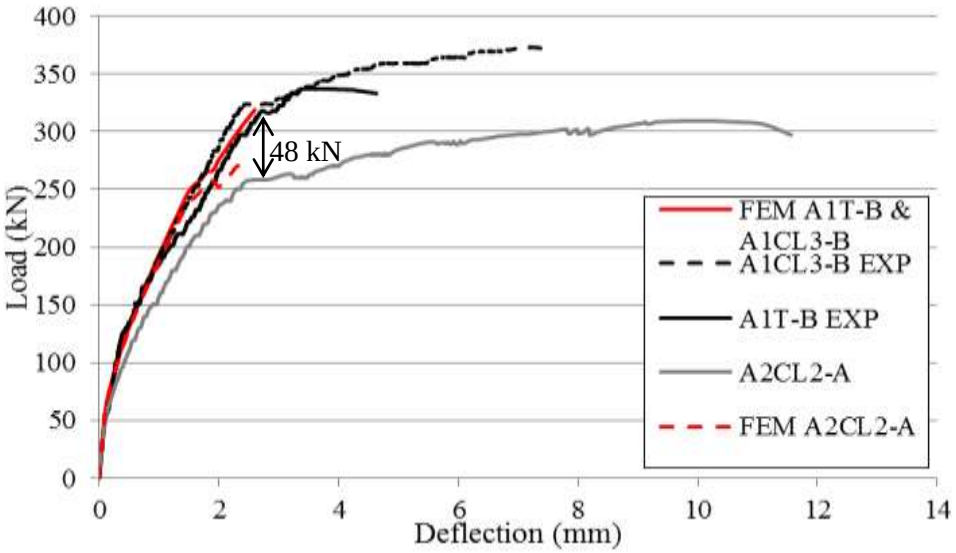

Figure 15 Experimental vs FE numerical model load-deflection curves for non-shear-repaired beams A1CL3-B , A2CL2-A and A1T-B

Figure 15, shows good agreement in the load-deflection behaviour between FE numerical models and experimental results. Although full numerical convergence was not obtained at this point, and capturing the post-yielding behaviour for RC beams failing in shear is difficult to achieve for this point since several new cracks are forming and, at the same time, the old existing cracks are changing their status. Figure 15 shows also that taking into account the steel corrosion for both tensile steel bars and steel stirrups in the FE numerical models led to a reduction of 48 kN in the yielding-moment capacity of the corroded RC beam A2CL2-A (56 kN loss of yielding-moment capacity was found experimentally). The same yielding capacity for both beams A1T-B and A1CL3-B was obtained as the corroded beam A1CL3-B has no corrosion at the edge where the shear failure. The crack pattern of the non-shear-repaired beams was obtained using FEMIX code and it is presented in figure 16.

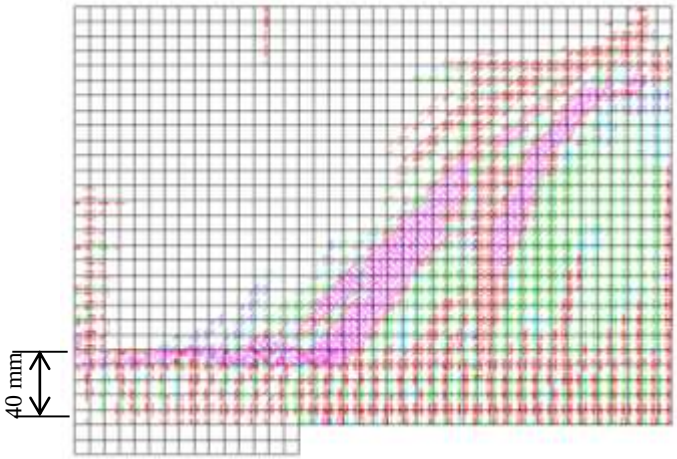

Figure 16 FE crack pattern of the non-shear-repaired beams (in pink colour: crack completely open; in red colour: crack in the opening process; in cyan colour: crack in the reopening process; green colour: crack in the closing process; in blue colour: closed crack).

The open diagonal shear cracks shown (see figure 16) presents the modes of failure for both beams non-shear-repaired with NSM obtained by the FE numerical model which coincides with what was found experimentally (see figure 6), the diagonal cracks continued to be horizontal near the support at the tensile steel bars location (40mm from the cover).

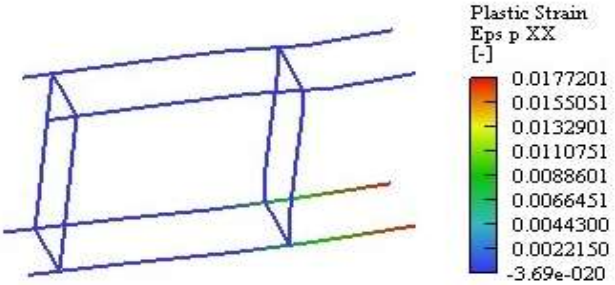

Figure 17 maximum strain values in the steel bars for the non-shear repaired beam A1CL3-B

The numerical FE model showed that the maximum reached strain value in the tensile bars of the corroded beam A1CL3-B was 0.02 (shown in figure 17) which is still less than the ultimate reduced strain value of the corroded steel bars 0.04, so for this point the steel corrosion did not lead to a brittle failure of the corroded steel bars neither experimentally nor in the numerical model which is different from the behaviour of corroded RC beams in bending.

4.2 Load-deflection curves and failure modes for RC beams shear repaired with NSM CFRP rods (A1CL3-SB and A1T-SB)

Figure 18 shows the FE numerical load-deflection curves for both models created for beams repaired in shear with NSM along with the experimental ones, the results show a good agreement between the behaviors of the four curves in terms of yielding capacity difference due to the corrosion found at the middle of the beam which represents 12% of loss of cross section and led to 12% loss in yielding capacity even though the full convergence was not achieved for both models due to the formation of the new cracks while the old cracks were changing their status at the same time i.e. (reopening or reclosing cracks).

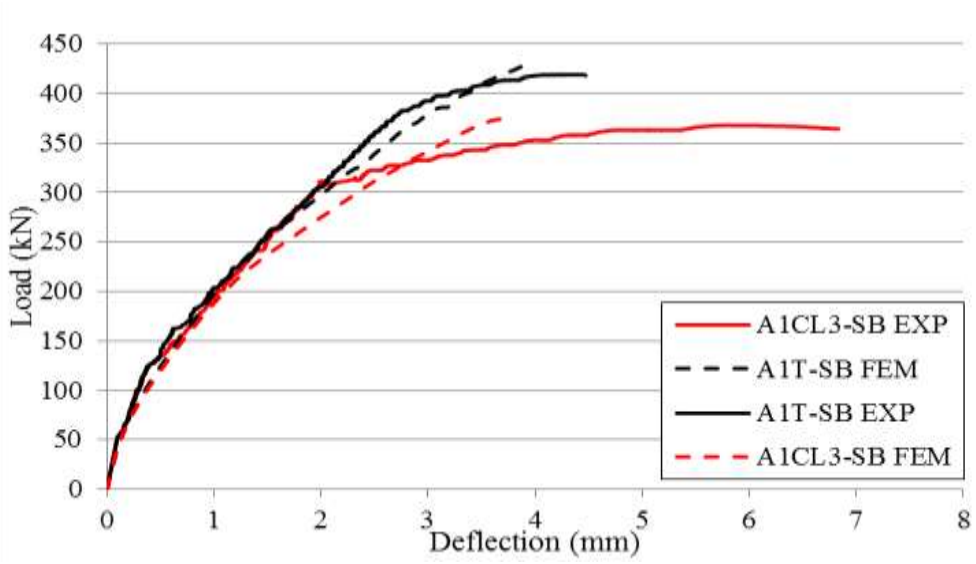

Figure 18 Experimental vs FE numerical model load-deflection curves for shear-repaired beams A1CL3-SB and A1T-SB

The crack patterns were obtained of the FE numerical model for 3-dimensional planes, the x-y plane shown in figure 19 shows a large purple open crack occurred at the middle of the beam, the same effect of shear strengthening with NSM CFRP rods was captured in the FE numerical model as for non-shear repaired beam the model failed in diagonal tension mode of failure with large shear cracks while for shear-repaired beam the mode of failure changed to large flexural cracks at the middle of the beam as shown in figure 19.

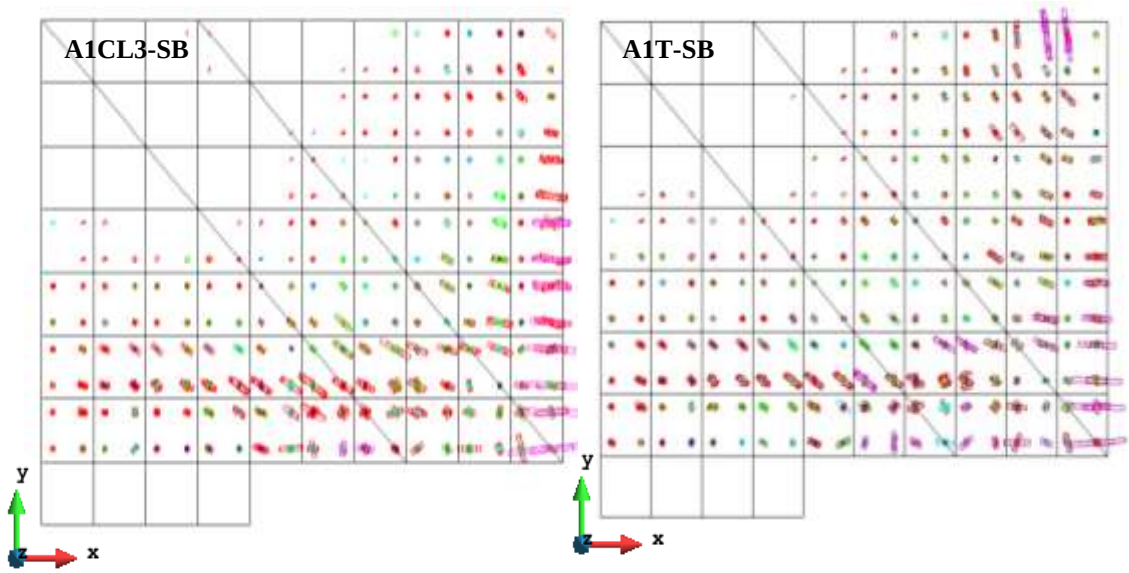

Figure 19 FE crack patterns of the shear repaired beams in x-y plane (in pink colour: crack completely open; in red colour: crack in the opening process; in cyan colour: crack in the reopening process; green colour: crack in the closing process; in blue colour: closed crack).

For x-z and y-z planes crack patterns shown in figure 20, some open cracks were observed at the middle and bottom of the beams while other open cracks located at the bottom of the beams near the support.

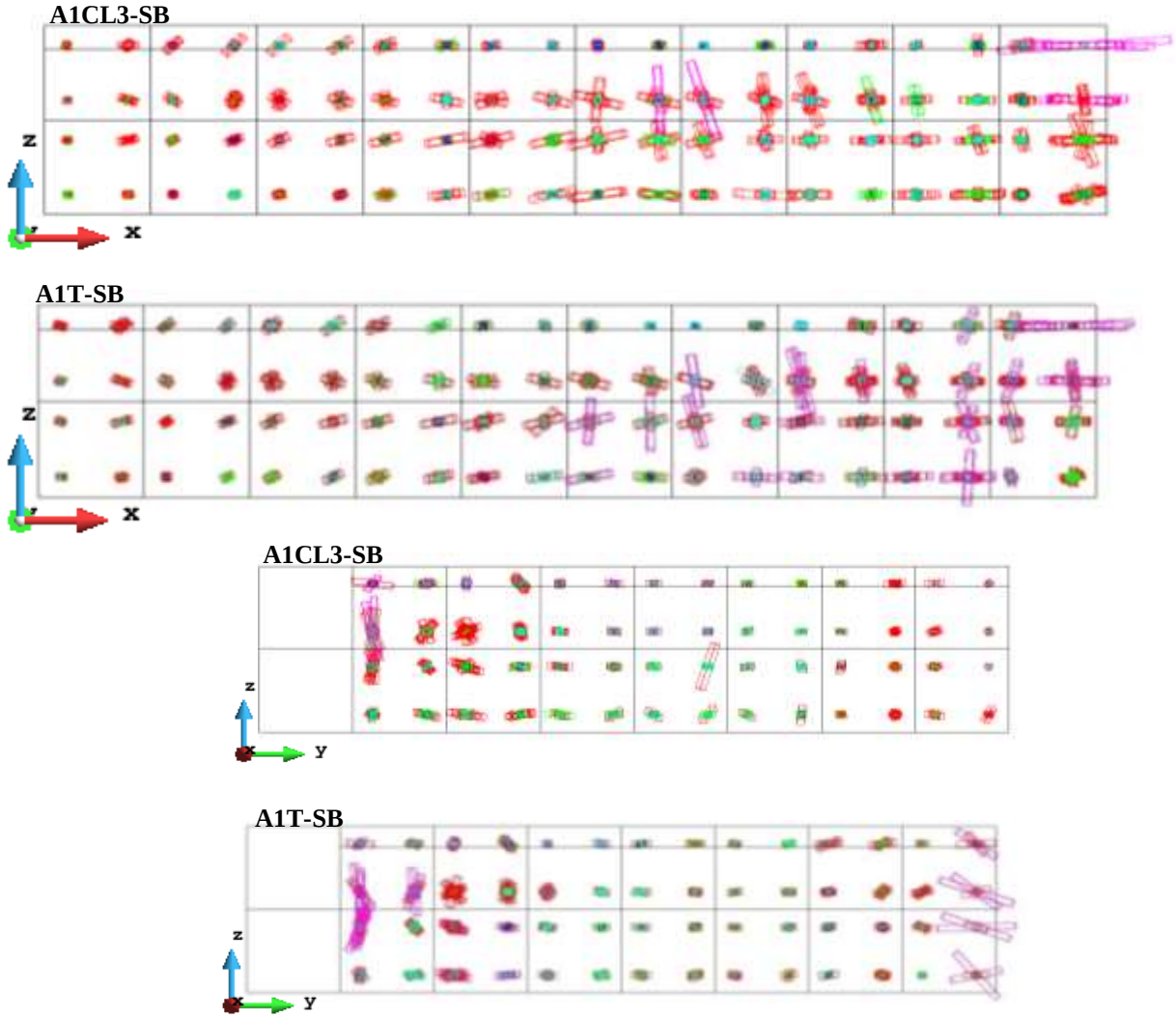

Figure 20 FE crack patterns of the shear repaired beams in x-z & y-z planes (in pink colour: crack completely open; in red colour: crack in the opening process; in cyan colour: crack in the reopening process; green colour: crack in the closing process; in blue colour: closed crack).

The shear strength contribution provided by a system of NSM FRP strips to a RC beam has been evaluated throughout the loading process by fulfilling equilibrium, kinematic compatibility, and constitutive laws of both the materials consisting the model and the bond between those materials (38,39). Bianco et al. (20) proposed a predictive model in order to investigate the NSM shear strengthening contribution, it was found that the contribution of the NSM laminates is limited by concrete tensile fracture along their available bond length, it was found also that the concrete around each NSM CFRP strip was not necessarily capable of

carrying the stresses transferred to it, it could fracture in a semi-conical surface. By reducing the laminates spacing, their semi-conical surfaces overlap (shown in figure 21 (a)) which allows the interaction between laminates to be easily accounted and the resulting concrete failure surface was almost parallel to the web face of the beam. The same crack patterns were found for the shear-repaired beams with NSM CFRP rods studied in this paper (A1T-SB and A1CL3-SB), as for the bottom and the edge of the beams there were visible splitting cracks (separation of the concrete sides including the NSM CFRP rods) which matches the predictive model proposed by Bianco et al. (20).

Figure 21 (a) shows a section parallel to the shear crack plane which presents the semi conical fracture surfaces of concrete due to excessive stresses of the approach proposed by Bianco et al. (20), figure 21 (b) and (c) presents the splitting cracks happened at the bottom and the edge of the shear-repaired beams A1T-SB and A1CL3-SB.

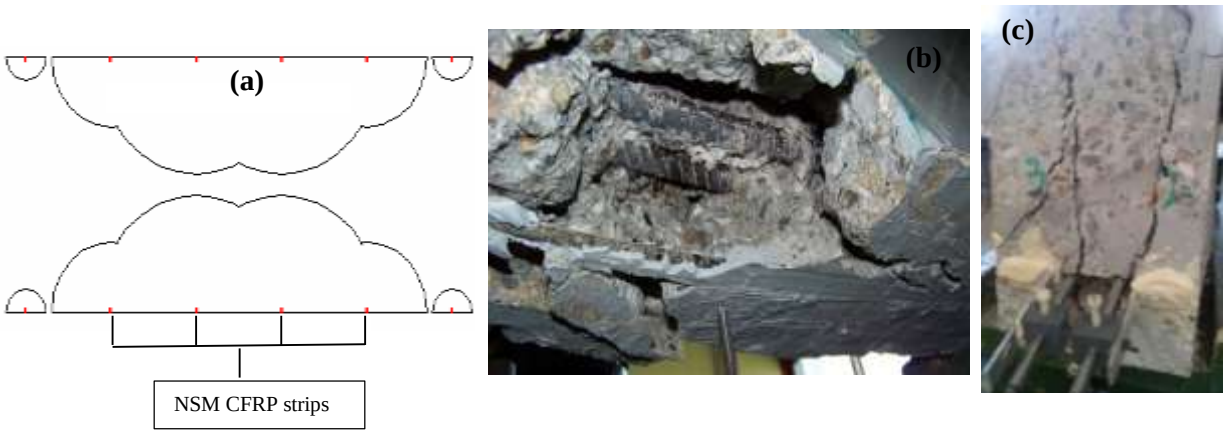

Figure 21 (a) Section parallel to the crack plane for the theory of the failure mode proposed by Bianco et al. 24. (b) Splitting cracks at the bottom of the shear repaired beams A1CL3-SB and A1T-SB. (c) Splitting cracks at the edge of the shear repaired beams A1CL3-SB and A1T-SB

5. Conclusions

According to the results found in this paper, the following conclusions can be drawn:

1. The comparison between the FE numerical predictions and the experimental results showed a satisfactory level of accuracy of the proposed model in terms of capturing the load-deflection curves and the crack patterns.
2. The loss of cross section of steel bars was well captured by the FE numerical models by capturing the same reduction of the yielding capacity occurred experimentally.

3. The effectiveness level of the NSM technique was limited by the semi conical effect of each NSM CFRP rod contribution and the non-repaired mid span point of the SB beams which led to splitting cracks happened at the middle of the RC beams strengthened in shear.
4. A FE numerical model which takes into account both the interaction between the NSM CFRP rods and the concrete, and the bond-slip relationship between concrete and corroded steel bars is required in the future.

REFERENCES

1. Tayeh BA, Abu Bakar B, Megat Johari M, Voo YL. Mechanical and permeability properties of the interface between normal concrete substrate and ultra high performance fiber concrete overlay. Constr Build Mater. 2012;36:538–48.

2. Andrade C, Alonso C, Garcia D, Rodriguez J. Remaining lifetime of reinforced concrete structures: Effect of corrosion on the mechanical properties of the steel. 1991;

3. Al-Sulaimani G, Kaleemullah M, Basunbul I. Rasheeduzzafar,(1990)"Influence of corrosion and cracking on bond behaviour and strength of reinforced concrete members" ACI Structural Journal, 87 (2), 220-231. ASTM G1. 1990;

4. Rodriguez J, Ortega L, Casal J. Load carrying capacity of concrete structures with corroded reinforcement. Constr Build Mater. 1997;11(4):239–48.

5. Chung L, Najm H, Balaguru P. Flexural behavior of concrete slabs with corroded bars. Cem Concr Compos. 2008;30(3):184–93.

6. Azad AK, Ahmad S, Azher SA. Residual strength of corrosion-damaged reinforced concrete beams. ACI Mater J. 2007;104(1).

7. Torres-Acosta AA, Navarro-Gutierrez S, Terán-Guillén J. Residual flexure capacity of corroded reinforced concrete beams. Eng Struct. 2007;29(6):1145–52.

8. Xia J, Jin W, Li L. Shear performance of reinforced concrete beams with corroded stirrups in chloride environment. Corros Sci. 2011;53(5):1794–805.

9. Wang X-H, Li B, Gao X-H, Liu X-L. Shear behaviour of RC beams with corrosion damaged partial length. Mater Struct. 2012;45(3):351–79.

10. Wang X-H, Gao X-H, Li B, Deng B-R. Effect of bond and corrosion within partial length on shear behaviour and load capacity of RC beam. Constr Build Mater. 2011;25(4):1812–23.

11. Zhu W, François R, Coronelli D, Cleland D. Effect of corrosion of reinforcement on the mechanical behaviour of highly corroded RC beams. Eng Struct. 2013;56:544–54.

12. Khan I, François R, Castel A. Experimental and analytical study of corroded shear-critical reinforced concrete beams. Mater Struct. 2014;1–15.

13. De Lorenzis L, Nanni A. Shear strengthening of reinforced concrete beams with near-surface mounted fiber-reinforced polymer rods. ACI Struct J. 2001;98(1).

14. Islam AA. Effects of NSM CFRP bars in shear strengthening of concrete members. ASCE; 2009. p. 1–14.

15. Rizzo A, De Lorenzis L. Behavior and capacity of RC beams strengthened in shear with NSM FRP reinforcement. Constr Build Mater. 2009;23(4):1555–67.

16. Dias SJ, Barros JA. Performance of reinforced concrete T beams strengthened in shear with NSM CFRP laminates. Eng Struct. 2010;32(2):373–84.

17. Omran HY, El-Hacha R. Nonlinear 3D finite element modeling of RC beams strengthened with prestressed NSM-CFRP strips. Constr Build Mater. 2012;31:74–85.

18. Nanni A, Di Ludovico M, Parretti R. Shear strengthening of a PC bridge girder with NSM CFRP rectangular bars. Adv Struct Eng. 2004;7(4):297–309.

19. Barros JA, Baghi H, Dias SJ, Ventura-Gouveia A. A FEM-based model to predict the behaviour of RC beams shear strengthened according to the NSM technique. Eng Struct. 2013;56:1192–206.

20. Bianco V, Barros JA, Monti G. A new approach for modelling the NSM shear strengthening contribution in reinforced concrete beams. J Compos Constr. 2007;

21. Almassri B, Kreit A, Al Mahmoud F, Francois R. Behaviour of corroded shear-critical Reinforced Concrete beams repaired with NSM CFRP rods. Compos Struct. 2014;

22. Rots JG, De Borst R. Analysis of mixed-mode fracture in concrete. J Eng Mech. 1987;113(11):1739–58.

23. Suryanto B, Nagai K, Maekawa K. Modeling and analysis of shear-critical ECC members with anisotropic stress and strain fields. J Adv Concr Technol. 2010;8(2):239–58.

24. Sena Cruz JM, Barros JA, Gettu R, Azevedo ÁF. Bond behavior of near-surface mounted CFRP laminate strips under monotonic and cyclic loading. J Compos Constr. 2006;10(4):295–303.

25. Barros JAO, Baghi H, Dias SJE, Ventura-Gouveia A. A FEM-based model to predict the behaviour of RC beams shear strengthened according to the NSM technique. Eng Struct. 2013 Nov;56(0):1192–206.

26. Barros JA, Costa IG, Ventura-Gouveia A. CFRP flexural and shear strengthening technique for RC beams: experimental and numerical research. Adv Struct Eng. 2011;14(3):551–71.

27. Castel A, François R, Arliguie G. Mechanical behaviour of corroded reinforced concrete beams—Part 1: experimental study of corroded beams. Mater Struct. 2000;33(9):539–44.

28. Vidal T, Castel A, François R. Corrosion process and structural performance of a 17 year old reinforced concrete beam stored in chloride environment. Cem Concr Res. 2007;37(11):1551–61.

29. Kreit A, Al-Mahmoud F, Castel A, François R. Repairing corroded RC beam with near-surface mounted CFRP rods. Mater Struct. 2011;44(7):1205–17.

30. Almassri B, Kreit A, Mahmoud FA, François R. Mechanical behaviour of corroded RC beams strengthened by NSM CFRP rods. Compos Part B Eng. 2014;64:97–107.

31. Dang VH, François R., Coronelli D., Shear behaviour and load capacity of short reinforced concrete beams exposed to chloride environment, European Journal of Environmental and Civil Engineering, to be published 2015.

32. François R, Khan I, Dang VH. Impact of corrosion on mechanical properties of steel embedded in 27-year-old corroded reinforced concrete beams. Mater Struct. 2013;46(6):899–910.

33. Zhu W, François R. Effect of corrosion pattern on the ductility of tensile reinforcement extracted from a 26-year-old corroded beam. Adv Concr Constr. 2013;1(2):121–37.

34. Apostolopoulos C, Papadakis V. Consequences of steel corrosion on the ductility properties of reinforcement bar. Constr Build Mater. 2008;22(12):2316–24.

35. Cairns J, Plizzari GA, Du Y, Law DW, Franzoni C. Mechanical properties of corrosion-damaged reinforcement. ACI Mater J. 2005;102(4).

36. Almusallam AA. Effect of degree of corrosion on the properties of reinforcing steel bars. Constr Build Mater. 2001;15(8):361–8.

37. Du Y, Clark L, Chan A. Residual capacity of corroded reinforcing bars. Mag Concr Res. 2005;57(3):135–47.

38. Bianco, V. "Shear strengthening of RC beams by means of NSM FRP strips: Experimental evidence and analytical modeling." Ph.D. thesis, Dept. of Structural Engrg. and Geotechnics, Sapienza Univ. of Rome, Italy. 2008.

39. Bianco V, Barros JA, Monti G. Bond model of NSM-FRP strips in the context of the shear strengthening of RC beams. J Struct Eng. 2009;135(6):619–31.